JOURNAL OF COMPUTATIONAL PHYSICS 94, 419–436 (1991)

Inverse Problem in Incompressible, Irrotational Axisymmetric Flow

SURYA PRASAD G. DINAVAHI* AND S.-K. CHOW†

Westinghouse R&D Center, Pittsburgh, Pennsylvania

Received February 27, 1989, revised February 2, 1990

An "inverse" problem to find the body shape given the surface velocity distribution in axisymmetric irrotational flow is formulated. The body surface is represented by a vortex sheet. An iterative, interactive computer program to compute the body shape starting from an assumed shape is developed. The obtained body shapes and the corresponding surface velocity distributions for three test cases are presented.

INTRODUCTION

The "inverse" problem solution procedure involves finding the geometry of a body given the velocity or pressure distribution on its surface. This is distinct from the "direct" problem in which the flow field around a given body is calculated. Sometimes in aerodynamic design problems, it becomes necessary to find a body shape with a certain surface velocity distribution. One can address this problem by trial and error, i.e., by solving the direct problem for several body shapes and observing which one of them gives the required characteristics. However, this is a tedious and time-consuming process and requires considerable amount of expertise from the investigator. Hence, it becomes desirable to have a solution procedure to solve the inverse problem, thus eliminating the trial and error in design problems. In the current study, it is assumed that flow is axisymmetric, incompressible, and irrotational.

PREVIOUS STUDIES

With the aid of high-speed computers, several numerical methods for solving axisymmetric-flow inverse-problems are reported to have been successfully developed in recent years. Bristow [1] uses a surface-source distribution to generate the flow and the surface of an unknown body configuration. The body shape and the source distribution are determined using a Lagrangian type error

* Presently with AS&M Inc., NASA Langley Research Center, Hampton, VA 23666.
† Presently with Westinghouse Nuclear and Advanced Technology Division, Monroeville, PA.

0021-9991/91 $3.00

minimization technique via an iterative calculation procedure. This solution technique minimizes the difference between a predefined surface tangential velocity distribution and the calculated velocity distribution based on the updated body shape and source distribution.

Zedan and Dalton [2–4] use an axial source distribution to generate the body and the flow. They utilize the stream function and the calculated velocities due to the axial source distribution to update the shape of the body, through an iterative procedure. The algorithm of their method is much simpler than that due to Bristow.

Fernandez [5] also utilizes the stream function approach in his mathematical model. However, he uses a surface source distribution instead of an axial source distribution. He formulates the problem in terms of "source-rings," and adapts a higher-order singularity technique to improve the accuracy and efficiency of the solution. Converged numerical solutions are obtained for several bodies having smooth surfaces. Based on the results of the test cases, Fernandez claimed that his method has a faster convergence rate than does Bristow's method.

Aside from the three numerical methods just cited, there have also been a number of other methods for solving the inverse problem of some special cases, employing various techniques. Several of these are included with the references listed at the end of this paper [6–11].

Problem Formulation

Consider a closed stream surface S which is symmetric about the z axis and is generated by a vortex sheet, see Fig. 1. A uniform flow is assumed to be moving in the negative z direction. Denote the tangential velocity on the surface by U_s. Since the surface S is a stream surface, the relative normal velocity on it has to be zero. The vortex sheet may be considered as formed by a series of "vortex rings" coaxial with the z axis.

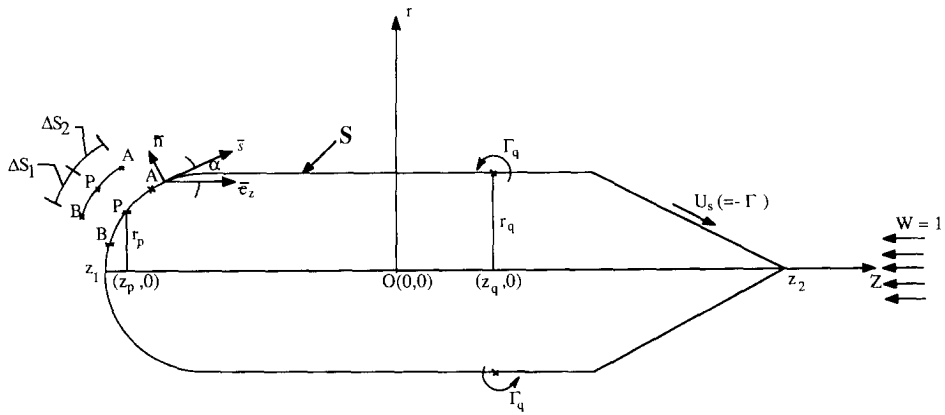

Fig. 1. Definition sketch.

By setting the tangential velocity on the inside of the surface S represented by a vortex sheet to zero, the result obtained is

$$\Gamma(q) = -U_s(q), \tag{1}$$

where $\Gamma(q)$ is the strength of the vortex ring at any point q on S. Satisfying the zero tangential velocity on the inside surface of a closed body represented by a vortex sheet, the zero normal velocity on the external body surface is automatically satisfied (see Appendix A).

A definition sketch for a vortex ring and the flow pattern generated by the ring

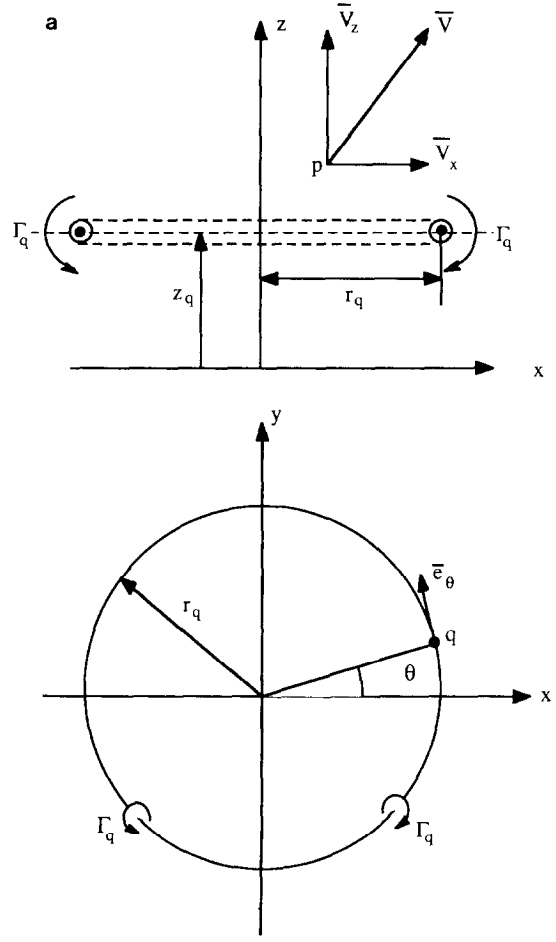

FIG. 2. (a) Definition sketch for a vortex ring. (b) Stream lines in the x–z plane due to a vortex ring coaxial with the z axis.

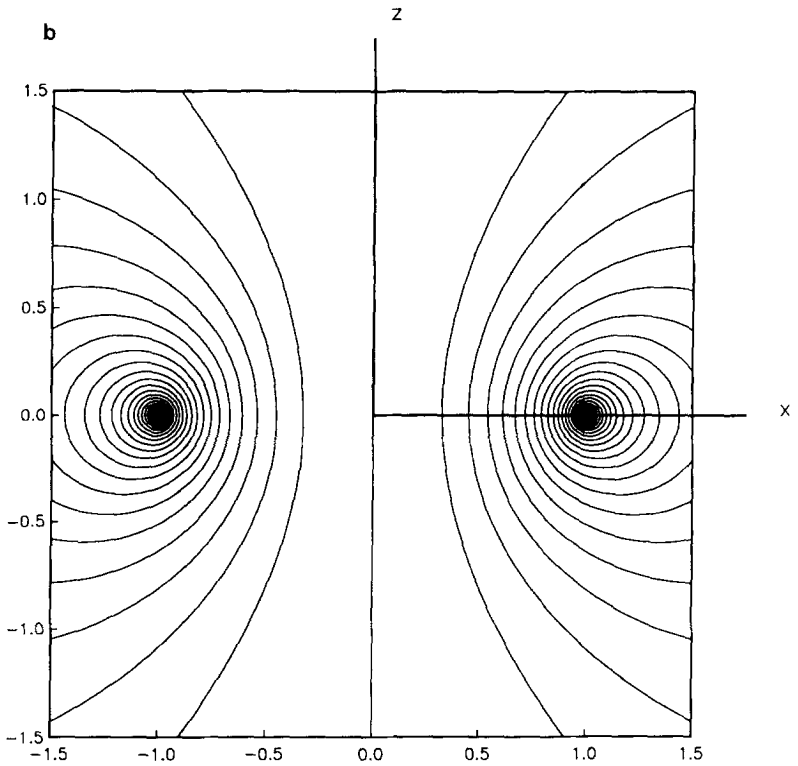

FIG. 2—*Continued.*

in x–z plane are shown in Fig. 2. The following expression for the stream function of a vortex ring given by Lamb [12] is used,

$$\Psi_v(p, q) = \frac{1}{2\pi}(r_1 + r_2)[K(\lambda) - E(\lambda)], \tag{2}$$

where $\Psi_v(p, q)$ is the stream function at a point $P(r_p, z_p)$ due to a unit strength vortex ring of radius r_q, situated at z_q, perpendicular to z axis, and

$$r_1 = \sqrt{(z_p - z_q)^2 + (r_p - r_q)^2} \tag{3}$$

$$r_2 = \sqrt{(z_p - z_q)^2 - (r_p - r_q)^2} \tag{4}$$

$$\lambda = \frac{r_2 - r_1}{r_2 + r_1} \tag{5}$$

$$K(\lambda) = \int_0^{\pi/2} \frac{d\phi}{\sqrt{1 - \lambda^2 \sin^2 \phi}} \tag{6}$$

$$E(\lambda) = \int_0^{\pi/2} \sqrt{1 - \lambda^2 \sin^2 \phi}. \tag{7}$$

Here $K(\lambda)$ and $E(\lambda)$ are complete elliptic integrals of the first and second kind, respectively.

The stream function due to an oncoming uniform stream of speed W is given by

$$\psi_w = -\tfrac{1}{2} W r_p^2. \tag{8}$$

The resultant stream function at any point p due to the uniform flow and the vortex sheet is

$$\psi_v(p) = -\tfrac{1}{2} W r_p^2 + \int_s \Gamma(q)\, \psi_v(p, q)\, ds_q. \tag{9}$$

In the above equation, ds_q is the arc length at point q in the meridional plane. Since S is a stream surface, we have $\Psi(p) = 0$, for a point p on S, giving

$$r_p^2 = \frac{2}{W} \int_s \Gamma(q)\, \psi_v(p, q)\, ds_q. \tag{10}$$

The above is a nonlinear integral equation in terms of the unknown body radius r_p. There are no known existence or uniqueness theorems available regarding the solutions to the above equation, to the authors' knowledge. However, as already outlined before, several numerical techniques are available to solve the inverse problem. Following the same spirit, we develop a numerical technique in the following sections.

Solution Procedure

Given U_s, the tangential velocity on the surface, the radius r of S may be obtained through an iterative procedure starting with an assumed profile in the following manner,

$$(r_p^2)^{k+1} = \frac{2}{W} \int_s \Gamma(q)\, \psi_v^k(p, q)\, ds_q, \tag{11}$$

where k is the iteration number. Note that the surface S as determined from (11) not only has a tangential velocit distribution identical to the pre-defined velocity distribution U_s, but also automatically satisfies the Neumann boundary condition (i.e., no flow can penetrate through the surface), since, by definition, it is the stream surface $\Psi = 0$.

The vortex-ring stream function given by (2) contains a mathematical singularity as the point q approaches p, i.e., as $q \to p$, $\lambda \to 1$, and $K(\lambda) \to \infty$. Even though the integral in (11) is improper, it is integrable and is finite. The integral has to be evaluated analytically in the neighborhood of the singularity. The procedure is outlined below. Let A and B be the two end points of an arc-segment Δs on which the

singularity point P is located, see Fig. 1. Let the arc lengths AP and BP be Δs_1 and Δs_2, respectively, and $\Delta s_p = \Delta s_1 + \Delta s_2$. Let z_1 and z_2 be the two extremities of the surfaces S on the z axis. Equation (11) may then be expressed as

$$(r_p^2)^{k+1} = \frac{1}{\pi W}\left\{\int_{z_1}^{B} + \int_{B}^{A} + \int_{A}^{z_2}\right\} \Gamma(q)\{(r_1 + r_2)[K(\lambda) - E(\lambda)]\}^k \, ds_q$$

$$= \frac{1}{\pi W}(I_1 + I_2 + I_3)^k, \tag{12}$$

where I_1, I_2, and I_3 are the integrals from z_1 to B, B to A, and A to z_2, respectively. I_1 and I_3 are singularity free and so can easily be evaluated numerically. Only I_2 contains an integrable singularity at the point P. We will now evaluate I_2 analytically for a small arc length Δs_p,

$$I_2 = \int_B^A \Gamma_q (r_1 + r_2)[K(\lambda) - E(\lambda)] \, ds_q$$

$$\simeq \Gamma_p \int_B^A (r_1 + r_2)[K(\lambda) - E(\lambda)] \, ds_q \tag{13}$$

as $q \to p$,

$$r_1 \to 0 \tag{14}$$

$$r_2 \to 2r_p \tag{15}$$

$$\lambda \to 1 \tag{16}$$

$$E(\lambda) \to 1, \tag{17}$$

and

$$K(\lambda) \to \ln \frac{4}{\sqrt{1 - \lambda^2}} = \ln \frac{2(r_1 + r_2)}{\sqrt{r_1 r_2}}$$

$$\simeq \frac{3}{2} \ln 2 + \frac{1}{2} \ln r_p - \frac{1}{2} \ln r_1. \tag{18}$$

Substituting Equations (14) to (18) in (13) (see Appendix B), we obtain

$$I_2 \simeq \Gamma_p r_p \{[3 \ln 2 + \ln r_p - 1](\Delta s_1 + \Delta s_2)$$

$$- (\Delta s_1 \ln \Delta s_1 + \Delta s_2 \ln \Delta s_2)\}. \tag{19}$$

This expression for I_2 is valid as long as $r_2 \simeq 2r_p$ and $r_2 \gg r_1$. Since the integrals of (11), I_1, I_2, and I_3 are all functions of Γ_q and r_q, we may write (11) as

$$(r_p^2)^{k+1} = f(\Gamma_q, r_q^k). \tag{20}$$

COMPUTER ALGORITHM

Various techniques have been tried for solving the above iteration formula. This iteration formula was found to be extremely slow in convergence. Among the several techniques tried, the weighting factor approach seems to be the most satisfactory one. Consider that a converged set of r's has been obtained. We then have

$$(r_p^2)^k - f(\Gamma_q, r_q^k) = 0. \tag{21}$$

Combining (20) and (21) yields

$$\begin{aligned}(r_p^2)^{k+1} &= (1+M) f(\Gamma_q, r_q^k) - M(r_p^2)^k \\ &= F(M, \Gamma_q, r_q^k),\end{aligned} \tag{22}$$

where M is a weighting factor such that $M \geqslant 0$. This is the equation that has been used in the present investigation. The adaptation of the weighting factor has immensely improved the convergence rate of calculation.

An interactive computer program is developed to solve the above equation in an iterative manner. This has the capability to display the body shape on the terminal in order to allow the investigator to observe the body shape after each iteration, and to gain experience in selecting the weighting factor to be used. As mentioned before, the weighting factor M has to be such that $M \geqslant 0$. The reason for this will be clear if we re-write the iteration formula (22) in the form,

$$(r_p^2)^{k+1} = f(\Gamma_q, r_q^k) - M[(r_p^2)^k - f(\Gamma_q, r_q^k)]. \tag{23}$$

Say that in the kth iteration $(r_p^2)^k > f(\Gamma_q, r_q^k)$. Then, in the next iteration, r_p^2 has to be corrected such that it becomes smaller. Since the bracketed term is greater than zero, M has to be greater than or equal to zero. It can be argued similarily when $(r_p^2)^k < f(\Gamma_q, r_q^k)$. A flow chart showing the computation procedure is shown in Fig. 3.

As indicated in the flow diagram, a prescribed velocity (or pressure) distribution, $U_s(q)$, which is numerically equal to the vortex strength Γ_q, is the input for this program. The z_q's are given, but the r_q's are unknown. A closed surface of arbitrary configuration may be assumed as the initial shape for the unknown surface which is to be determined. A weighting factor M is then selected (initially M should be small, say, $M \leqslant 3$). A new set of stream-surface radii is calculated by (22), and the configuration so obtained is displayed and visually examined. The interactive computer program provides several options for the investigator. The investigator may select a new M value for the next iteration, call the direct-problem subroutine to compute the velocity distribution (if desired), continue, or terminate the calculation. The investigator may instruct the program to "go back" to the previous iteration and use a different M value to repeat the calculation. This last-mentioned option is particularily useful when some "kinks" appear on the updated surface

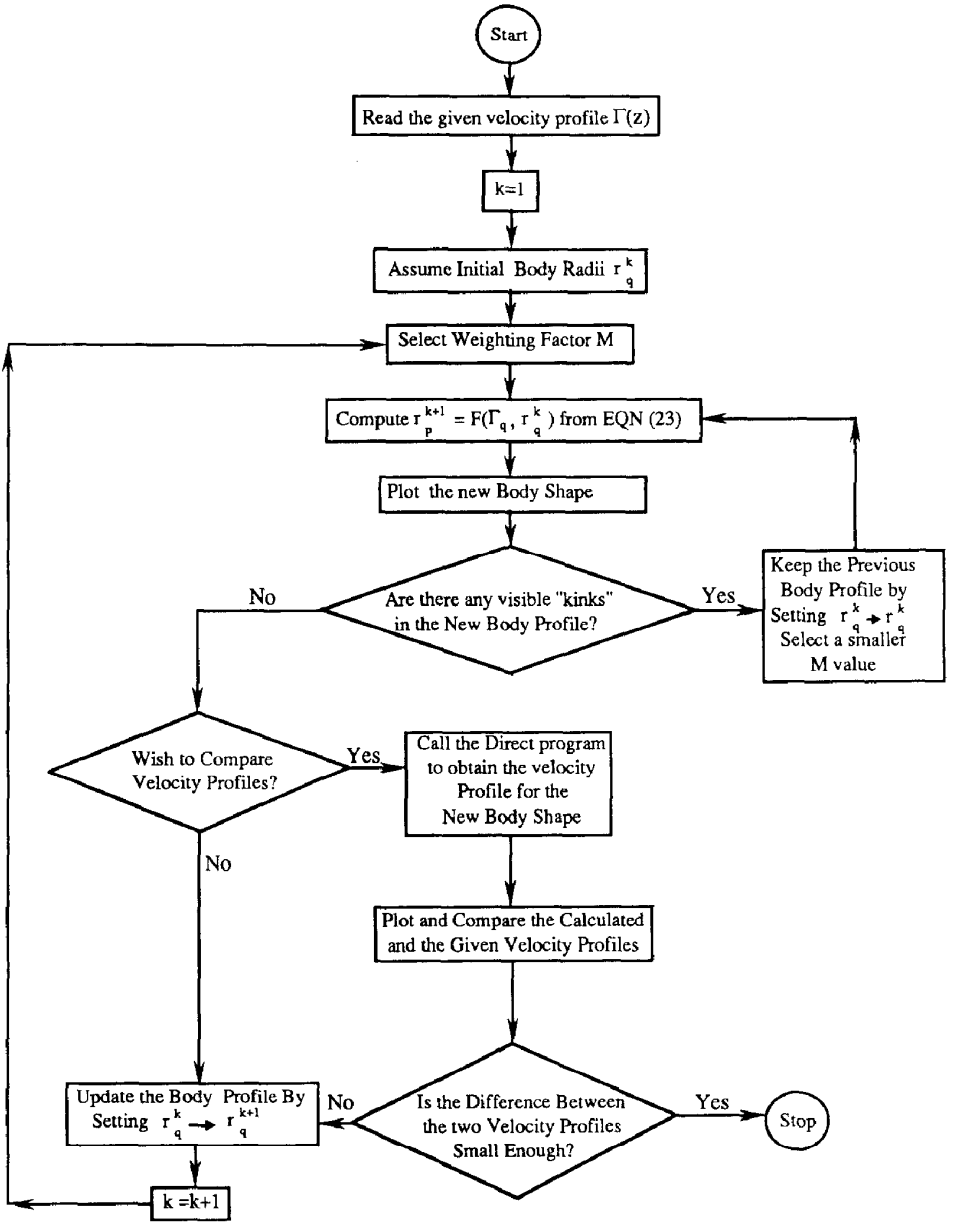

FIG. 3. Flow diagram for the inverse problem using an interactive procedure.

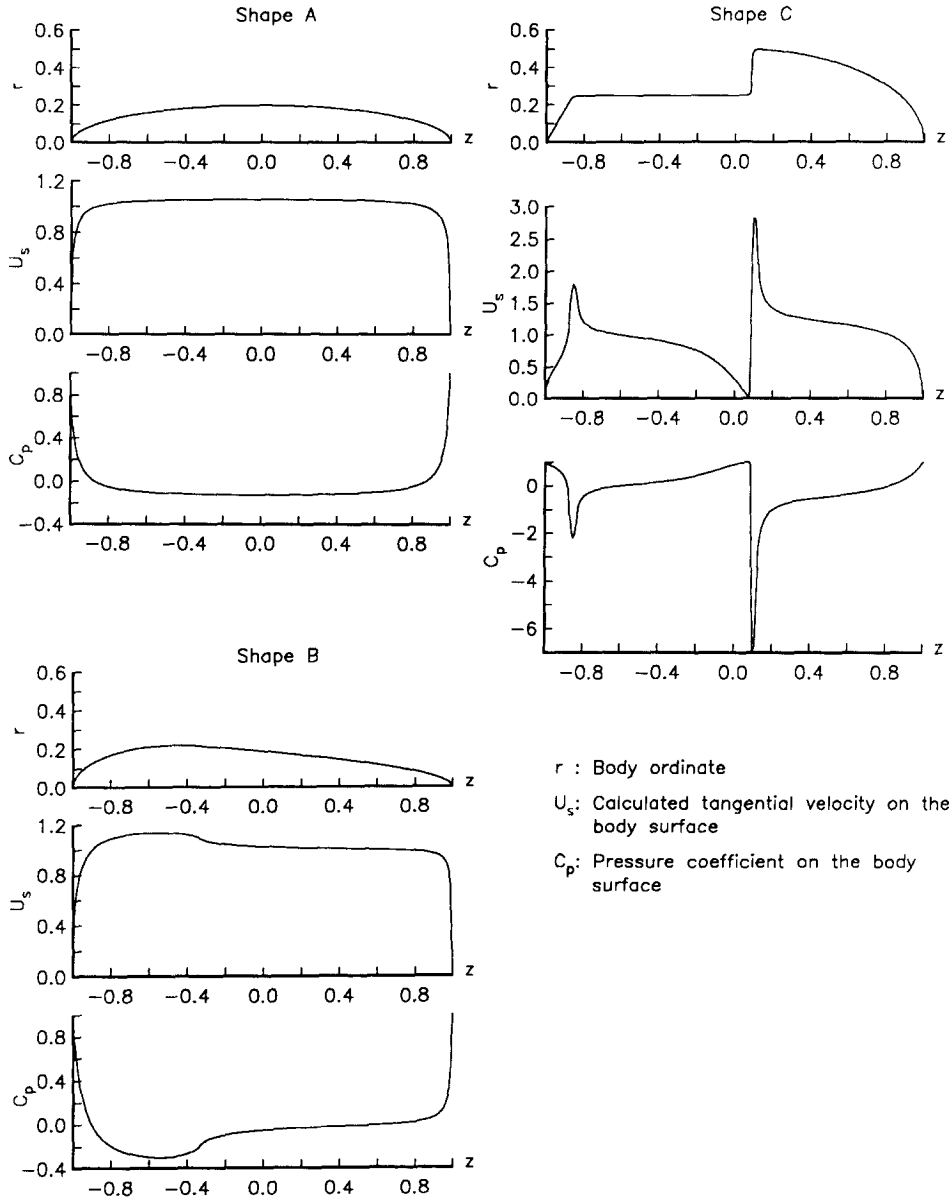

FIG. 4. Assumed body shapes, their calculated velocity profiles and pressure coefficients.

profile due to the over-amplification effect of a larger-than-desired weighting factor used. (This sometimes happens when $M > 6$.) With this option, the investigator can "erase" the undesired results, go "backward" one iteration, and use a smaller M value to restart the computation. The solution may be considered converged when the maximum difference between the calculated r_p's from two successive iterations, or the maximum relative error between the computed and the prescribed velocity distributions, is smaller than a preselected allowable value.

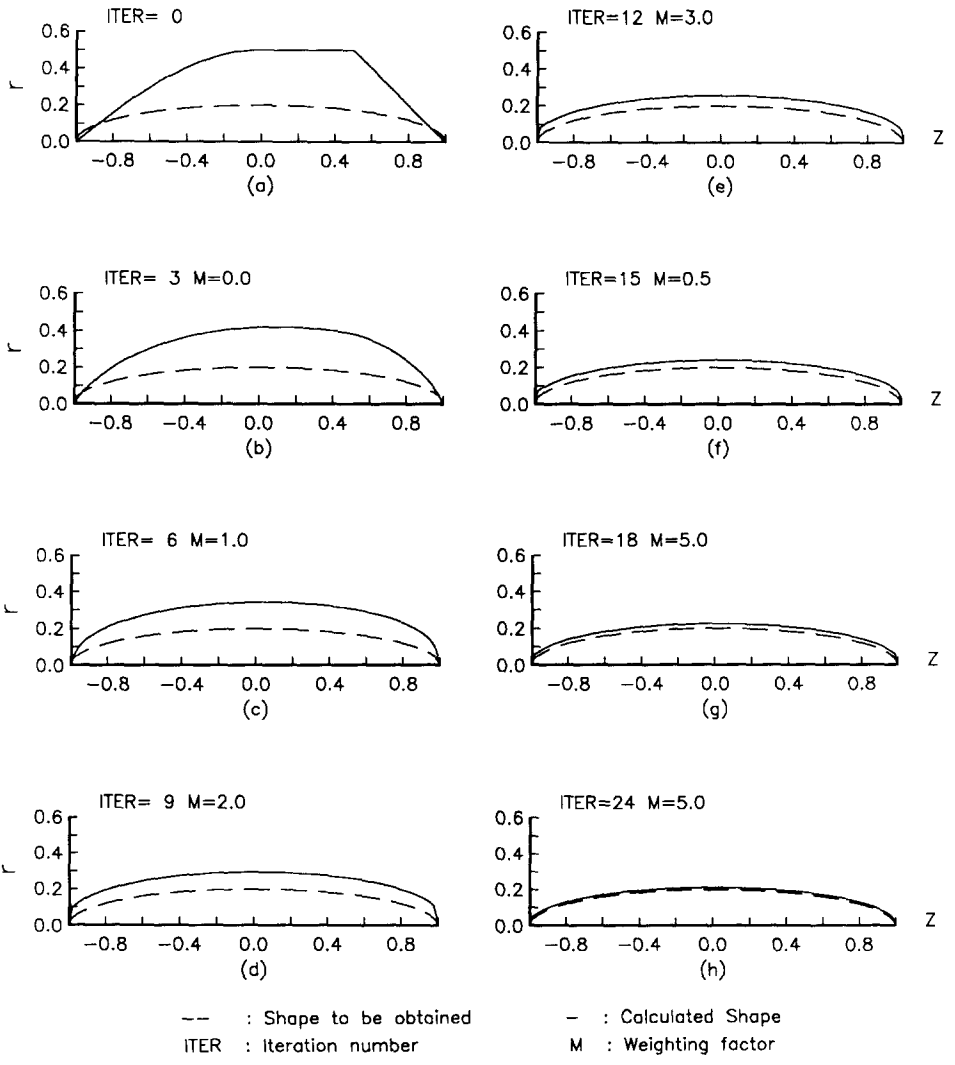

FIG. 5. Comparison between the actual shape and the calculated shape for body A as the iterations progress.

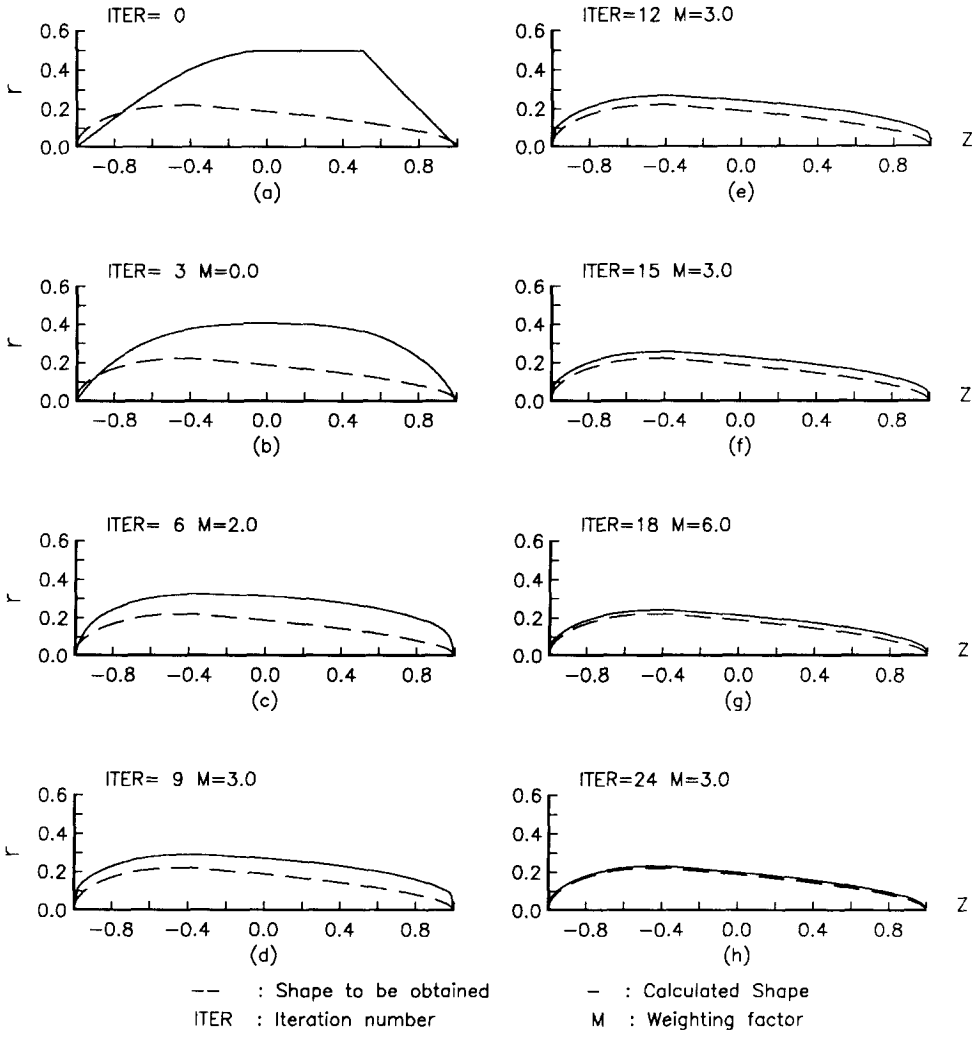

FIG. 6. Comparison between the actual shape and the calculated shape for body B as the iterations progress.

RESULTS

Three surface configurations, A, B, and C, which are shown in Fig. 4, have been used as test shapes to validate the vortex–sheet inverse-problem solution method developed. Shape A is a spheroid of slenderness ratio of 5:1, shape B is a streamlined form, and shape C is similar to the body shape used by Bristow [1] which has rapid changes in the surface slope and body radius. The velocity and pressure distributions for these bodies calculated by the vortex-sheet direct-problem

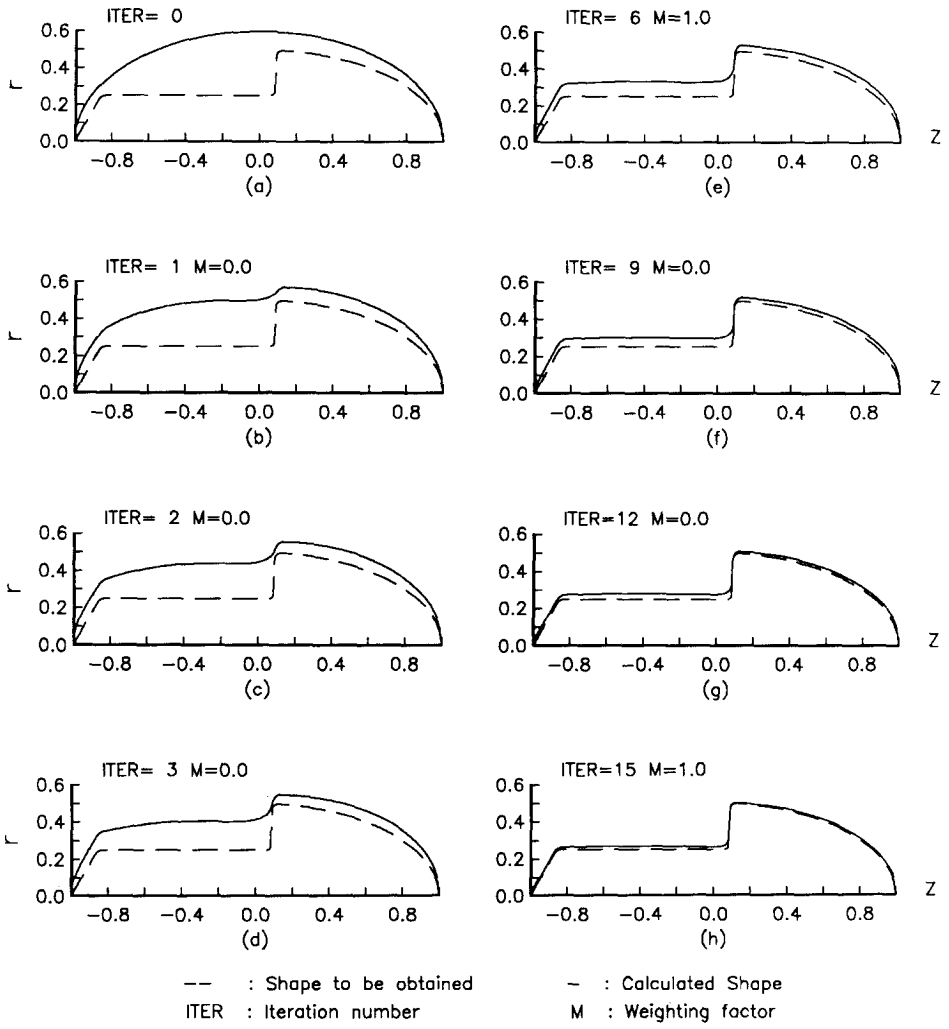

FIG. 7. Comparison between the actual shape and the calculated shape for body C as the iterations progress.

method are also shown in Figure 4. These velocity distributions are used as the "predefined" velocity distributions in the inverse-problem calculations. The oncoming flow is assumed to have unit velocity, i.e., $W = 1$.

The stream-surface shapes obtained by the inverse method through the iterations are shown in Figs. 5–7. The solid-line profiles are the calculated shapes. These figures show how the unknown shapes with predefined surface velocity (or pressure) distributions are obtained progressively by the vortex-sheet inverse-problem solution procedure. Successive iteration results are not shown; rather,

some intermediate results are shown. The iteration number and the weighting factor used in that iteration are shown for each shape drawn.

Figure 8 shows the converged solutions obtained for the three body shapes, and comparisons of the calculated and the prescribed velocity distributions. In the present examples the iterations are considered to be converged when the relative error between the calculated and the given velocity distributions is less than or equal to 1%. The good agreement between the calculated and the given velocity profiles confirms the validity of the new inverse-problem method developed (See Fig. 8).

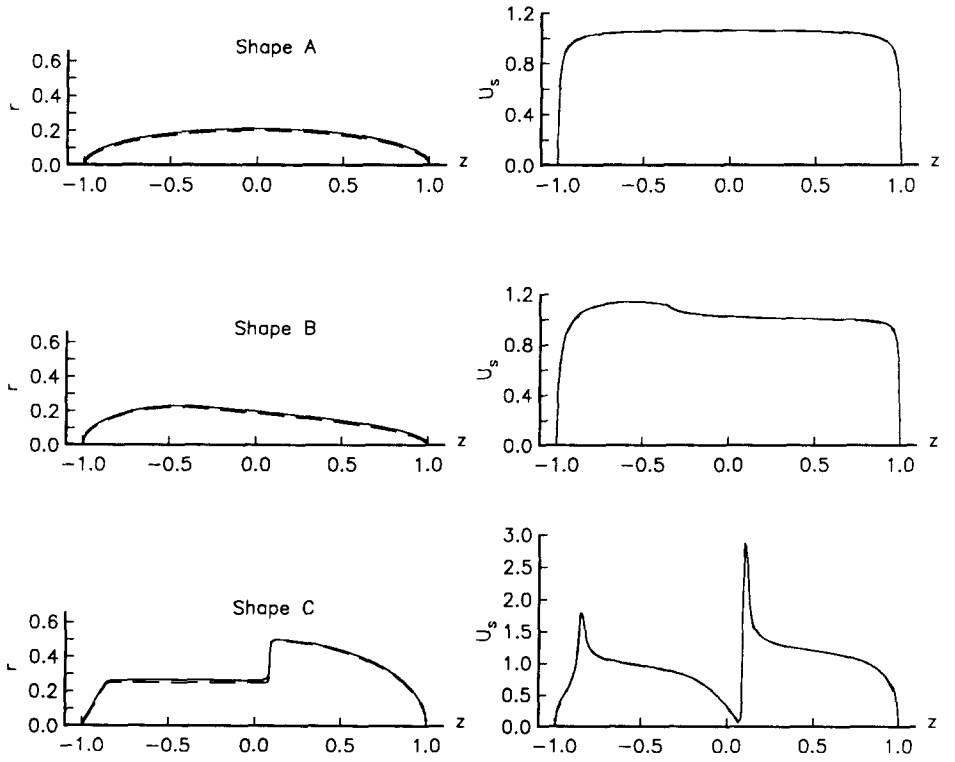

r : body ordinate
— actual
– calculated (converged)

U_s : tangential velocity on the body surface
— calculated from the actual body shape
– calculated from the converged body shape

FIG. 8. Comparison between the actual values and the converged values.

Conclusions

A vortex-sheet method to solve the axisymmetric inverse problem is developed and is successfully demonstrated in solving the shown test cases. This program can be used as an efficient tool in the design process. The advantage of this method is that it eliminates the calculation of the direct problem at every iteration (thus reducing calculation time considerably); instead, it uses the given velocity. The singular integral that arises in the problem formulation has been integrated analytically as shown in Appendix B.

A few words need to be said about the use of the weighting factor M used to speed up convergence. Unfortunately, there is no set rule or procedure which the authors could prescribe in using M other than that one has to be judicious. It is found through experience that the value of M used should not be too large (6 in this case). In the present examples, either the starting body shape or the actual body shape has sharp corners. In such a case, use of too large a value for M sometimes produces kinks in the calculated body profile. For such occasions, the facility to go back one step and redo the calculation with a smaller M value is provided in the computer program. In the authors' opinion, one should use a value of 0 for M in the initial stages of the computation. This program is intended for use in finding an unknown body shape given the velocity profile. In such a situation, one should plot the calculated body shapes for two successive iterations to see if there is any change in the two calculations. If no change can be observed visually, one can increase the value of M to see if that produces any change in successive calculations (iterations). Once one is satisfied that even by using a moderately high value for M, there is no change between two successive iterations, then the direct problem should be called to calculate the velocity and this calculated velocity should be compared against the input.

As far as the uniqueness of the solutions is concerned, the derived integral equation in terms of the unknown body radius r_p is highly nonlinear. To the best of the authors' knowledge there are no uniqueness or existence proofs for this type of integral equation. From experience, it appears that, given a pressure/velocity distribution for which there is a unique body shape, the solution method seems to find that shape. The formulation however, requires that the given pressure/velocity distribution correspond to that of a closed body.

Appendix A: Vortex Sheet Approach

Let the surface of a closed body in a flow field be represented by a vortex sheet. Assume further that there are no singularities within the body. Let S^+ represent the external body surface and S^- represent the interior of the body surface as shown in Fig. A.1.

Theorem 1. *The condition that the body surface S^+ is a stream surface can be*

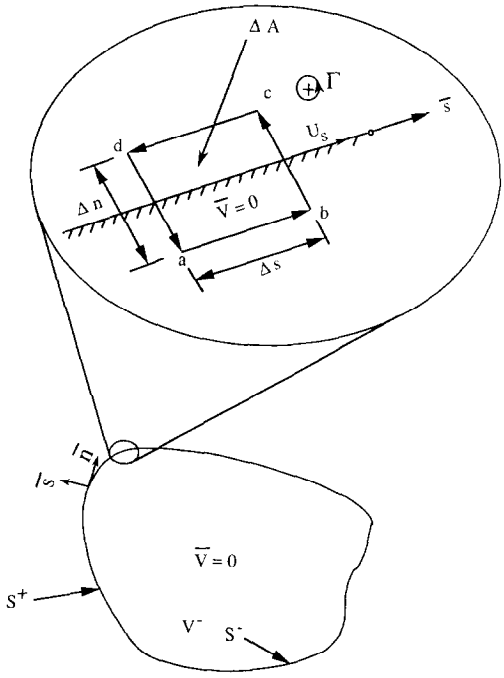

FIG. A.1. Vortex sheet approach.

satisfied by setting the tangential velocity on the interior (S^-) of the surface S^+ to zero.

Proof. Zero tangential velocity on the surface S^- implies that the velocity potential Φ is constant ($=C$) on the surface S^-. We have for the kinetic energy T of the fluid *within* the body,

$$T=\frac{1}{2}\rho\int_{V^-}(\nabla\Phi)\cdot(\nabla\Phi)\,dv=\frac{1}{2}\rho\int_{S^-}\Phi\frac{\partial\Phi}{\partial n}\,dS=\frac{1}{2}\rho C\int_{S^-}\frac{\partial\Phi}{\partial n}\,dS. \qquad (A.1)$$

But the integral $\int_{S^-}(\partial\Phi/\partial n)\,dS$ is zero since there are no singularities within the body. This implies that the kinetic energy of the fluid *within* the body is zero. Hence the fluid inside the body is at rest. So the normal velocity of the fluid on the interior of the body S^- is also zero. The normal velocity across a vortex sheet is continuous and hence the normal velocity on the exterior surface S^+ is also zero. Thus the body surface S^+ is a stream surface satisfying the no penetration condition. Q.E.D.

Under the above conditions, it can be shown that the vortex sheet strength is equal in magnitude to the tangential velocity on the body surface.

By the use of Stokes' theorem, the circulation around a closed circuit can be

shown equal to the flow of vorticity coming out of the area enclosed by that circuit (see Fig. A.1),

$$\int_{abcda} \mathbf{V} \cdot \mathbf{ds} = \iint_{\Delta A} \omega \, dA = \int_{\Delta s} \Gamma \, ds, \tag{A.2}$$

where Γ is the vortex sheet strength per unit length defined as

$$\lim_{\Delta n \to 0, \omega \to \infty} \omega \, \Delta n = \Gamma. \tag{A.3}$$

We then have

$$-U_s \, \Delta s = \Gamma \, \Delta s, \tag{A.4}$$

or

$$U_s = -\Gamma. \tag{A.5}$$

If the sign convention for either U_S or Γ is reversed, then we get the equality

$$U_s = \Gamma. \tag{A.6}$$

By setting the tangential velocity on the inside of the body surface to zero, an integral equation of the second kind in terms of the unknown vortex strength (also the tangential velocity) on the body surface is derived. A very highly accurate computer program to solve the direct problem is written and used to find the velocity distribution on the given body surface. The analytical solution for longitudinal flow past a spheroid is known. The tangential velocity is $U_s = (1 + k_{11}) \cos \alpha$, where k_{11} is the added mass of the spheroid in the longitudinal direction and α is the angle made by the tangent vector with the longitudinal axis. For a 5:1 spheroid as used in shape A, $k_{11} = 0.0591211$. The relative error in the calculated tangential velocity in the middle is 0.0014%. The relative error is no more than 0.1% in other areas except at the three or four end points where it climbs to 6.9%. This program can be made even more accurate at the end points but it is deemed accurate enough for the present purposes.

The preceding proofs and a more detailed account of the direct problem solution procedure can be found in the as yet unpublished class notes of Professor L. Landweber [13].

Appendix B: Treatment of the Singularity in the Inverse Problem

The elliptic integral $K(\lambda)$ in (13) has a logarithmic singularity as $q \to p$, i.e., as $\lambda \to 1$. This singularity becomes an integrable singularity if we assume that the vortex strength is constant over the segment BPA and equal to Γ_p. Substituting Eq. (14) to (18) in (13), we obtain

$$I_2 = \Gamma_p \int_B^A 2r_p \left[\tfrac{3}{2} \ln 2 + \tfrac{1}{2} \ln r_p - \tfrac{1}{2} \ln r_1 - 1\right] ds_q$$

$$= r_p \Gamma_p \int_B^A [3 \ln 2 - 2 + \ln r_p - \ln r_1]\, ds_q. \tag{B.1}$$

In the above equation as $q \to p$, $r_1 \to 0$ and the integrand becomes singular. Consider the integral

$$\int_p^A \ln r_1 \, ds_q, \tag{B.2}$$

where, by definition, $r_1 = \sqrt{(z_p - z_q)^2 + (r_p - r_q)^2}$ and is equal to the distance s measured along the straight line segment PA from the point P (see Fig. B.1). We then have

$$\int_p^A \ln r_1 \, ds = \int_0^{\Delta s_2} \ln s \, ds = [s \ln s - s]_0^{\Delta s_2} = \Delta s_2 \ln(\Delta s_2) - \Delta s_2, \tag{B.3}$$

since

$$\lim_{s \to 0} s \ln s = 0.$$

Hence, we have

$$I_2 = r_p \Gamma_p \left\{\int_B^P + \int_P^A\right\} [3 \ln 2 - 2 + \ln r_p - \ln r_1]\, ds$$

$$= \Gamma_p r_p \{[3 \ln 2 + \ln r_p - 1](\Delta s_1 + \Delta s_2)$$

$$- (\Delta s_1 \ln \Delta s_1 + \Delta s_2 \ln \Delta s_2)\}. \tag{B.4}$$

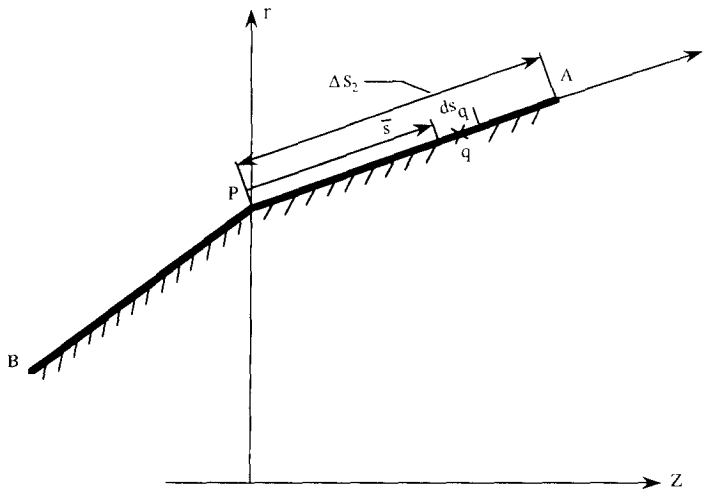

FIG. B.1. Singularity treatment.

ACKNOWLEDGMENTS

This work was done during 1982–1983 when the authors were with the Westinghouse R&D Center. The work was sponsored by the Westinghouse Marine Division as one of the approaches that would be used to determine the shape of the free-surface of a tail bubble formed at the end of an object launched underwater.

REFERENCES

1. D. R. BRISTOW, AIAA paper 74-520, 1974 (unpublished).
2. M. F. ZEDAN AND C. DALTON, *J. Hydronaut.* **12**, 41 (1978).
3. M. F. ZEDAN AND C. DALTON, "Higher-Order Axial Singularity Distributions for Potential Flow about Bodies of Revolution," in *Computer Methods in Applied Mechanics and Engineering* (North-Holland, Amsterdam, 1980), p. 295.
4. C. DALTON AND M. F. ZEDAN, *J. Hydronaut.* **15**, 48 (1981).
5. J. FERNANDEZ, The Pennsylvania State University Report No. TM79-125, 1979 (unpublished).
6. G. VIKTOROV AND MORGUNOV, Solution of the inverse problem for profile cascades on axisymmetric stream surfaces in a variable layer, translated from *Izvetsia Akad. Nauk. SSR Mekh. Zhidk. Gaza* **3**, 55 (1968).
7. V. M. IVCHENKO AND V. M. ROMAN, *Fluid Mechanics Sov. Res.* **1**, 121 (1972).
8. T. STRAND, *J. Aircraft* **10**, 651 (1973).
9. A. M. ANTONOV, *Dopov. Akad. Nauk. Ukr. RSR Ser. A.* **8**, 728 (1974).
10. S. D. KOSTRONOI AND A. A. LITVINENKO, *Izv. Vyssh. Uchebn. Zaved. Tekh.* **21** (1978).
11. L. ZANNETTI, *AIAA J.* **18**, 754 (1980).
12. H. LAMB, *Hydrodynamics*, 6th ed., (Dover, New York, 1945).
13. L. LANDWEBER, Hydrondynamics Class Notes, Iowa Institute of Hydraulic Research, The University of Iowa, Iowa City, IA, developed over the years 1970–1982 (unpublished).